

Pilot scale application of the Membrane Aromatic Recovery System (MARS) for recovery of phenol from resin production condensates

Frederico Castelo Ferreira^a, Ludmila Peeva^a, Andrew Boam^b,
Shengfu Zhang^b, Andrew Livingston^{a,*}

^a Department of Chemical Engineering and Chemical Technology, Imperial College London, Exhibition Road, London SW7 2AZ, UK

^b Membrane Extraction Technology Ltd., Sherfield building, Imperial College London, London SW7 2AZ, UK

Received 26 March 2004; received in revised form 6 August 2004; accepted 15 August 2004

Available online 8 February 2005

Abstract

This paper describes the application of the Membrane Aromatic Recovery System (MARS) to the recovery of phenol from wastewater streams arising from a phenolic resins production plant. These wastewater streams typically contain between 2 and 8 wt.% phenol, and their detoxification has a significant economical and environmental impact, since about 30% of the global phenol consumption is intended for phenolic resins synthesis (annual production of approximately 3 million metric tons resin). A MARS pilot plant unit operating in batch mode was installed at a United Kingdom resin manufacturing site, and average efficiencies of 94 and 84%, for the phenol extraction and the phenol recovery stages, respectively, were achieved. The final MARS product, an organic phase, composed of 77–80 wt.% phenol and 20–23 wt.% water, was recycled back to the original manufacturing process and successfully used as a reagent for resin production. The phenol content in the discharged wastewater stream was successfully reduced to 0.1–0.3 wt.%, sufficiently low to allow further detoxification by a destructive process, such as biotreatment or chemical oxidation. The influence of different parameters, such as stripping solution pH and neutralizing HCl solution concentration on the process performance was evaluated. Scale up effects on the mass transfer at the extraction stage were also analysed on the basis of the liquid film theory and the resistances in series approach.

© 2005 Elsevier B.V. All rights reserved.

Keywords: Phenol recovery; Phenolic resins production; Wastewater streams; MARS pilot plant; Scale up effects on the mass transfer

1. Introduction

Membrane Aromatic Recovery System (MARS) is a membrane process for recovery of organic acids and bases from wastewater streams, whose operating principles are illustrated in Fig. 1 and discussed elsewhere [1]. MARS was first applied to the recovery of phenol [1] and aniline [2] from synthetic wastewaters at laboratory scale with the MARS extraction stage configured in a continuous mode. The first MARS pilot scale unit was applied to recover aniline from an industrial wastewater effluent arising in a 4-nitrodiphenyl production process. Initially, the extraction stage was also operated in continuous mode [3]. In this application, the

wastewater flowed inside the membrane tubes and aniline accumulated in the stripping solution, outside the tubes, as anilinium. However, a solid precipitate present in the wastewater eventually blocked the tubes. To avoid this problem, the plant was reconfigured for batch operation, with the stripping solution flowing inside the membrane tubes, and wastewater batches on the outside of the membrane tubes.

Phenol is an aromatic acid, with a pK_a of about 10 and solubility of 8 wt.% in water at 25 °C. This compound is highly toxic and one of the EPA's priority pollutants [4]. Two of the main commercial applications for phenol are production of Bisphenol A and phenol-formaldehyde resins with, respectively, 37 and 30% of the global phenol consumption in 2001 [5]. Phenol and formaldehyde are the main reagents in the phenol-formaldehyde resin production process. One of the reaction products is water, which has to be removed

* Corresponding author. Tel.: +44 20 7594 5582; fax: +44 20 7594 5629.
E-mail address: a.livingston@imperial.ac.uk (A. Livingston).

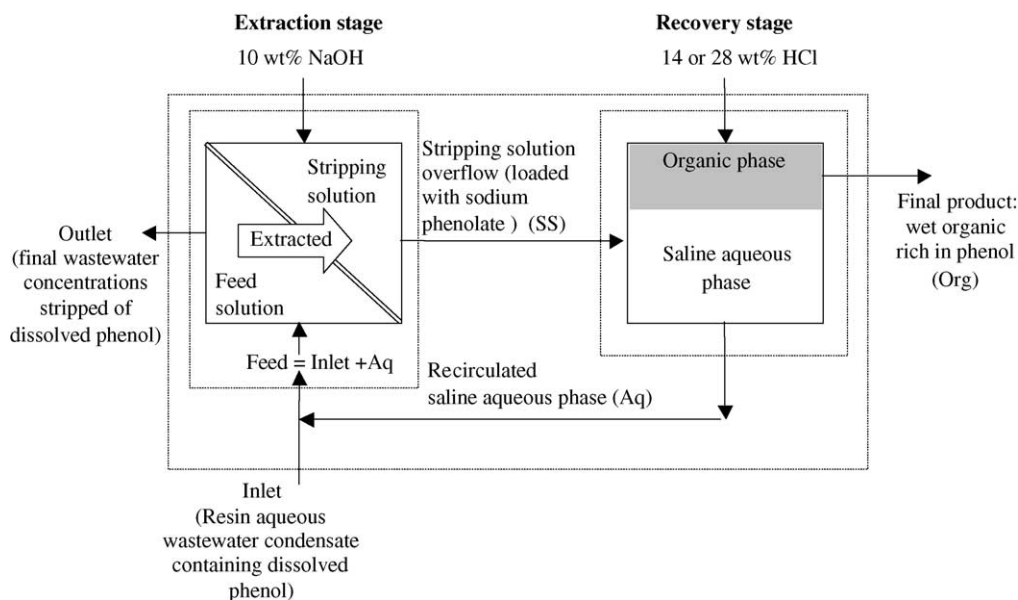


Fig. 1. Schematic diagram of the MARS operating principle.

from the crude resin mixture before further processing of the resin. The water can be removed by distillation, generating an aqueous phenolic condensate stream, containing phenol. The global production of phenolic resins reached 2.9 million metric tons in 2001, and therefore, the residual phenol recovery from the distillate has a major environmental and economical impact [5].

In the United Kingdom phenol-formaldehyde resin production plant studied in this work, the initial fraction of the distillate contains low concentrations of phenol and can be submitted directly to a destructive process. As the distillation temperature rises, the phenol content in the aqueous condensate increases and all the fractions with phenol concentrations between 0.5 and 8 wt.% are collected together giving

a main distillate fraction with an average content of 5 wt.% phenol, which is usually sent for an off-site disposal at a cost of $\$45\text{ t}^{-1}$ to $\$150\text{ t}^{-1}$. A small volume of the remaining bottom product is fed to a phase separator for phenol phase separation, and the residual aqueous phase, containing up to 8 wt.% phenol, is also sent to the off-site disposal.

This paper has three objectives: (i) report, for the first time, the application of the MARS process for recovery of phenol from a resin production condensates industrial pilot scale, (ii) evaluate the effect of lower HCl concentrations on performance of MARS, and (iii) study of scaling up effects on mass transfer.

The main objective of the present work is to investigate the potential replacement of the off-site phenol disposal stage

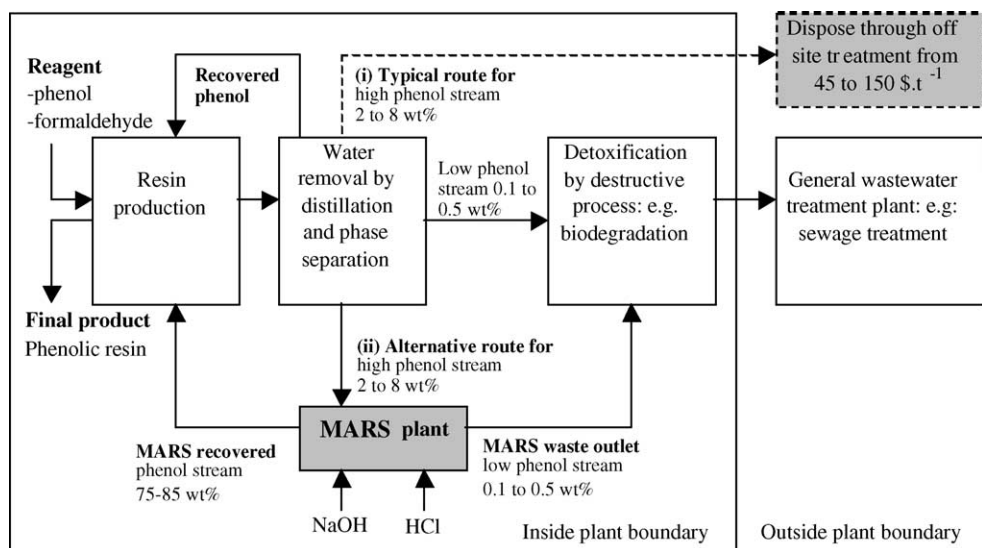


Fig. 2. Integration of MARS in a resin production process.

(Fig. 2) with the MARS process. In the proposed alternative route, the aqueous phenolic resin wastewater streams with 2–8 wt.% phenol are feed to the MARS process which, recovering as much phenol as possible, reduces the phenol concentrations to values low enough (e.g. 0.1–0.3 wt.%) to allow further downstream phenol detoxification by destructive processes, such as biodegradation or chemical oxidation. In the United Kingdom plant where the MARS trials were performed, the aqueous wastewater streams were produced in batches, and therefore, the MARS process was also applied in batch mode. The batch configuration has an added advantage in that it avoids potential membrane tube blockage by solid particles present in the wastewater.

2. Process performance analysis

2.1. Mass transfer equations

In this work, the theoretical analysis is based on the resistances in series approach and the liquid film theory. The overall mass transfer coefficient, based on a concentration driving force, is expressed as the sum of three mass transfer resistances in series: (i) the membrane resistance, (ii) the stripping solution liquid film resistance, and, (iii) the feed solution liquid film resistance. In the stripping solution, a chemical reaction takes place, which results in mass transfer enhancement, expressed by an enhancement factor, E :

$$\frac{1}{K_{ov}} = \frac{1}{k_f} + \frac{1}{k_m} + \frac{1}{Ek_s} \quad \text{with} \quad \frac{1}{k_m} = \frac{r_i \ln(r_o/r_i)}{P} \quad \text{and} \quad \frac{1}{k_g} = \frac{1}{k_f} + \frac{1}{k_m} \quad (1)$$

The effect of chemical reaction on the MARS mass transfer has been extensively studied elsewhere [6,7]. Calculations based on the Olander model [6] show that, for the conditions employed in this study, the term $1/Ek_s$ contributes with less than 1% to the overall mass transfer resistance $1/K_{ov}$ (see Appendix A for details). Therefore, it can be assumed that the chemical reaction enhancement completely eliminates the stripping solution liquid film resistance and Eq. (1) simplifies into Eq. (2).

$$\frac{1}{K_{ov}} = \frac{1}{k_f} + \frac{1}{k_m} \quad (2)$$

Eq. (3), describes feed solution bulk phenol concentration ($A_{f,b}$) over time, for a batch process, assuming the feed volume in the extraction tank (V_f) is constant, and a phenol flux based on (i) the overall mass transfer coefficient (K_{ov}), (ii) the membrane area (S_m) used and, (iii) a bulk concentration driving force, in which the neutral phenol concentration ($A_{s,b}$) in the bulk stripping solution is assumed

constant at a steady state value.

$$V_f \frac{dA_{f,b}^t}{dt} = -K_{ov} S_m (A_{f,b}^t - A_{s,b}) \quad (3)$$

The overall mass transfer coefficients are estimated from Eq. (4), an integrated form of Eq. (3):

$$\ln \left(\frac{A_{f,b}^t - A_{s,b}}{A_{f,b}^{t=0} - A_{s,b}} \right) = - \left(\frac{K_{ov} S_m}{V_f} \right) t \quad (4)$$

Assuming negligible neutral phenol concentration ($A_{s,b}$) in the bulk stripping solution, the driving force term becomes $A_{f,b} - A_{s,b} \approx A_{f,b}$ and Eq. (4) simplifies into Eq. (5). The accuracy of this assumption is discussed in Section 4.

$$\ln \left(\frac{A_{f,b}^t}{A_{f,b}^{t=0}} \right) = - \left(\frac{K_{ov} S_m}{V_f} \right) t \quad (5)$$

2.2. Extraction efficiencies, reagent ratios and dilution ratios

MARS performance is evaluated through an extraction efficiency (EE) and a recovery efficiency (RE). These parameters are defined based on the flow-sheet illustrated in Fig. 1.

$$EE = 1 - \frac{\text{phenol in the MARS outlet (kg)}}{\text{phenol fed to extraction tank (kg)}} = 1 - \frac{\text{Outlet}}{\text{Feed}} \quad (6)$$

which can also be expressed as:

$$EE = \frac{\text{phenol extracted (kg)}}{\text{phenol fed to extraction tank (kg)}} = \frac{\text{Ext}}{\text{Feed}} \quad (7)$$

$$RE = \frac{\text{phenol in the organic phase (kg)}}{\text{phenol in the stripping solution overflow (kg)}} = \frac{\text{Org}}{\text{SS}} \quad (8)$$

In the recovery stage, two phases are generated: (i) the phenol rich organic layer, which is the final MARS product, and, (ii) the aqueous saline layer. The saline layer ratio (SLR) compares the masses of these two phases:

$$SLR = \frac{\text{mass of saline aqueous phase (kg)}}{\text{mass of organic phase (kg)}} = \frac{\text{Aq}}{\text{Org}} \quad (9)$$

The aqueous saline layer produced in the recovery stage is circulated back to the extraction tank to remove any residual phenol. To evaluate the impact of this recirculation on the MARS process, two additional parameters are introduced, the stream and phenol dilution ratios (SDR and PDR, respectively), which are ratios between the recirculated aqueous saline phase and the aqueous phenolic wastewater arising from the resin production and fed to the MARS process as inlet.

$$\begin{aligned} \text{SDR} &= \frac{\text{mass of saline aqueous phase (kg)}}{\text{mass of resin wastewater condensate (kg)}} \\ &= \frac{A_q}{\text{Inlet}} = \frac{\text{Feed}}{\text{Inlet}} - 1 \end{aligned} \quad (10)$$

$$\begin{aligned} \text{PDR} &= \frac{\text{phenol in aqueous saline phase (kg)}}{\text{phenol in the resin wastewater condensate (kg)}} \\ &= \frac{\text{PhOH } A_q}{\text{PhOH Inlet}} = \frac{\text{PhOH Feed}}{\text{PhOH Inlet}} - 1 \end{aligned} \quad (11)$$

3. Experimental

3.1. Chemicals, analytical techniques and membrane material

Phenol and toluene concentrations were measured by GC analysis. Their aqueous solutions were diluted with distilled water and neutralised using HCl. The resulting aqueous solution was extracted with dichloromethane (DCM), and the DCM phase injected into the GC. The organic phase from phenol recovery was directly diluted in dichloromethane for phenol quantification, also by GC analysis. The coefficient of variation for these assays (over 5 measurements) was lower than 5% at 1000 mg L⁻¹ and the detection limit was established at 10 mg L⁻¹. Water content in the organic phase was measured by the Karl Fisher method giving a coefficient of variation less than 5% over five measurements for each sample. NaOH and HCl concentrations were assessed by titration, assisted by pH measurement. The membrane tube coils employed in this work had an internal diameter of 3 mm, a wall thickness of 0.5 mm, and a length of 100 m, and were composed of a cross-linked 70 wt.% polydimethylsiloxane polymer with 30 wt.% silica dioxide as filler.

Table 1

Operating parameters for phenol extraction at the pilot plant unit

Nr membrane coils	(a) 115, (b) 80
Membrane area	(a) 108.1 m ² , (b) 75.2 m ²
Coil membrane length	100 m
Internal membrane radius	1.5 mm
Membrane tube thickness	0.5 mm
Extraction temperature	(c) 50 °C, (d) 30 °C
Stripping solution pH	(e) 12.8–13.0, (f) 11.5
Extraction tank volume	1000 L
Feed volumes	648–785 kg
Inlet effluent volumes	377–685 kg
NaOH added to stripping	10.4 wt. %
HCl fed to wastewater	14 wt. %
HCl fed to recovery	(g) 14 wt. % (h) 28 wt. %

On batches: (a) 1–11, (b) 12–15, (c) 2–15, (d) 1, (e) 3–15, (f) 1 and 2, (g) 1–4, (h) 5–15.

3.2. Pilot plant equipment

A picture of the pilot plant installation, and a schematic diagram are shown in Figs. 3 and 4 and operating parameters are summarised in Table 1. The pilot plant unit is composed of three main tanks: the 1000 L membrane extraction tank, the stripping solution tank and the recovery vessel. Extra tanks are used as reservoirs for the reagent (HCl and NaOH) solutions and for the saline layer and stripping solution overflow solution. Phenol extracted from the feed solution through the membrane tube walls causes a pH drop in the stripping solution due to the neutralization reaction. To maintain the stripping solution at steady state phenol concentration and at a constant pH value, sodium hydroxide was added when required to the stripping solution tank, through a feed back loop connecting a pH probe to pump 6 (Fig. 4).

The membrane module was immersed inside the extraction tank. This module consists of a cubic cage holding

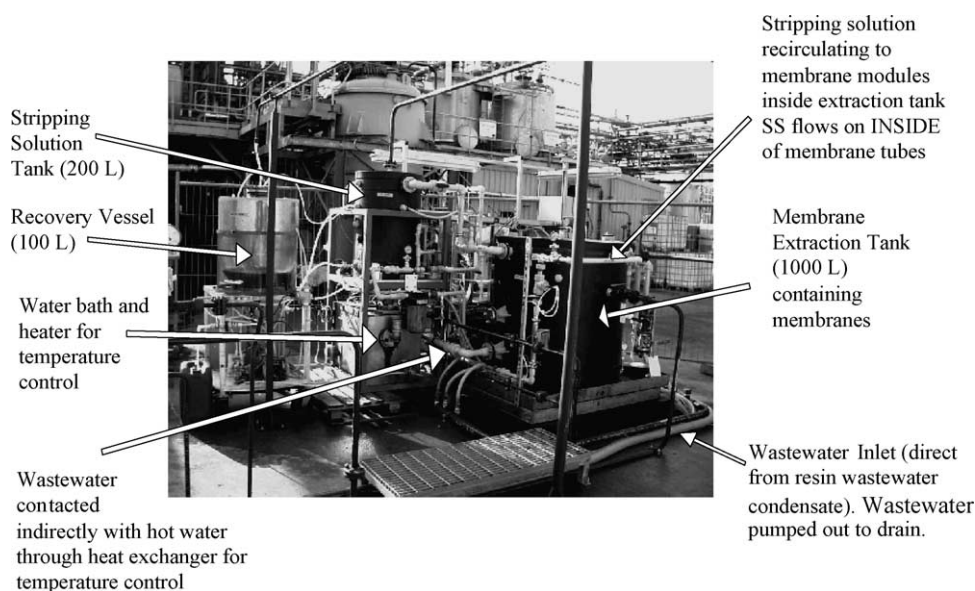


Fig. 3. Picture of the MARS pilot plant unit.

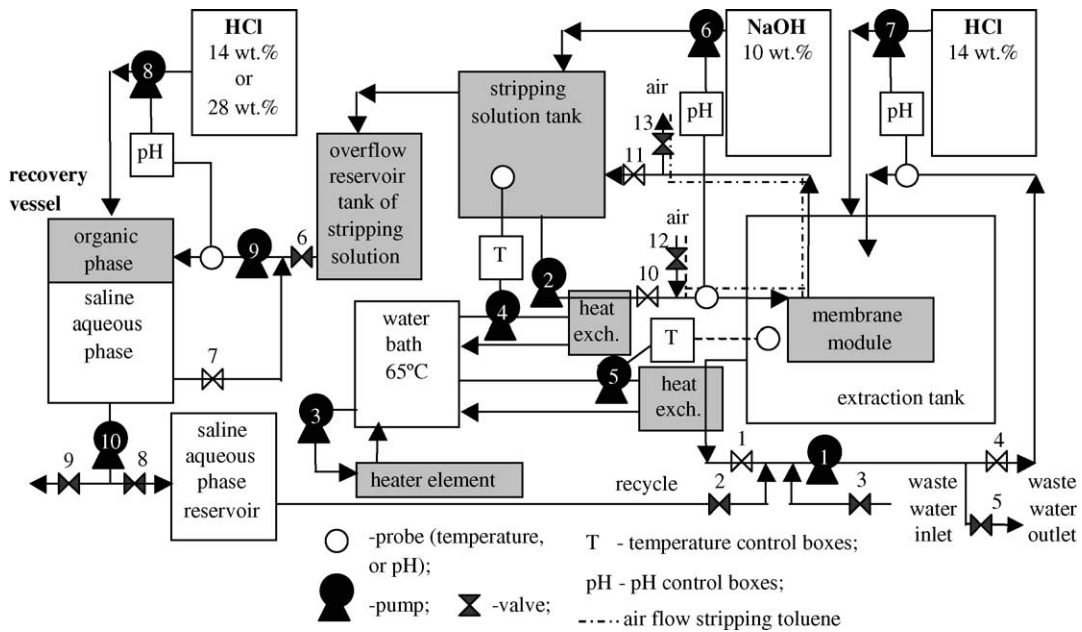


Fig. 4. Schematic diagram of MARS pilot plant unit.

several 100 m long membrane tube coils connected in parallel. Two membrane modules were used for phenol extraction trials and the differences between them are illustrated in Fig. 5. Module I consists of 115 coils of 100 m long membrane tube closely packed inside the cubic cage. Module II was divided into three sections, the two outer compartments were filled with 80 membranes coils in total (40 each) and the middle section was left void to provide better mixing of the feed solution in the extraction tank.

The stripping and feed solution temperatures were controlled at 50 °C by two feed back loops with temperature probes and pumps 4 and 5, circulating water pre-heated to 65 °C through two heat exchangers, as illustrated in Fig. 4. The feed solution pH was controlled at a value below 3 by

another feed back loop with a pH probe and pump 7, adding 14 wt.% HCl solution when required.

3.3. Pilot plant operation in batch mode

MARS was operated in sequential extraction and recovery batches. At the beginning of each extraction batch the 1000 L extraction tank was filled with a mixture of (i) the saline aqueous phase generated from the previous recovery batch and (ii) the industrial phenolic resin aqueous wastewater. At the end of an extraction batch, the wastewater stripped of phenol was discharged from the extraction tank and the phenol, removed from the wastewater and accumulated in the stripping solution overflow, was fed to the recovery batch.

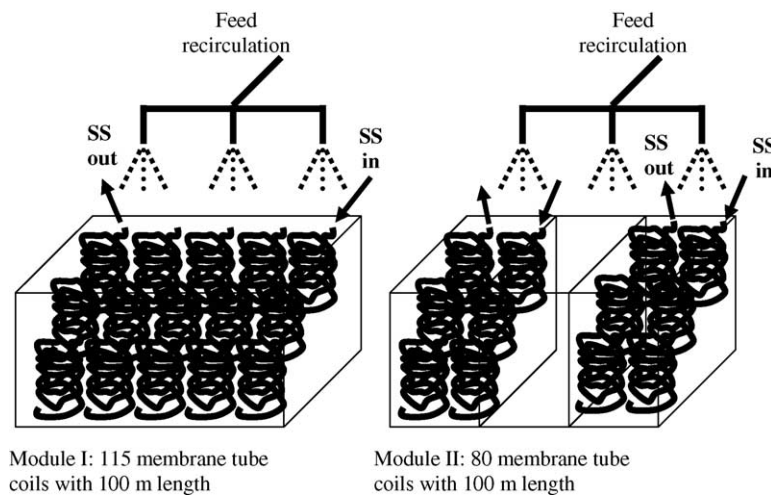


Fig. 5. Schematic diagram of the two membrane modules employed in the pilot plant unit.

Once this recovery batch is completed, the resulting aqueous saline layer was transferred to the next extraction batch, closing the cycle. This process was repeated many times. Cycle disruption occurred in extraction batches 1–3. In extraction batches 1 and 2, only the phenolic resin aqueous wastewater was fed to extraction. Extraction batch 3 included the two saline aqueous phases generated in recovery batches 2 and 1. Each extraction batch took about 46–48 h; module I was used for batches 1–11 and module II for batches 12–15.

Detailed scheme of the process operation and flows is presented in Fig. 4. Pump 1 was used, either to (i) recirculate the wastewater solution in the course of the batch extraction, ensuring the extraction tank is well mixed; or (ii) feed the extraction tank with phenolic wastewater and saline aqueous layer at the extraction batch start up. During initial MARS start-up, the stripping solution tank and the membrane tube lumens were filled with a stripping solution at steady state concentration, prepared by neutralizing a 10 wt.% NaOH solution with phenol to a pH value of 13. During the extraction, the stripping solution was recirculated via pump 2 between the stripping solution tank and the lumen of the membrane tubes at a flow rate of $1.5 \text{ dm}^3 \text{ h}^{-1}$ per tube.

As phenol was extracted, NaOH was added to maintain constant stripping solution pH. Since the concentration of NaOH being added is constant, this also results in a constant total phenol concentration at steady state in the stripping solution. The stripping solution generated overflowed from the stripping solution tank to a reservoir tank. Pump 9 was used either: (i) to transfer the stripping solution overflow to the recovery vessel or (ii) to promote good mixing during the stripping solution neutralization, which was performed by adding HCl (14 or 28 wt.%) until the pH in the recovery vessel became lower than 3. Due to the lower neutral phenol solubility in water, the solution separates into two phases: a phenol rich organic layer and an aqueous saline layer. After a settling time of 45–90 min, the saline aqueous phase was transferred to a reservoir tank and the recovered organic

phase was returned to the original phenolic resin production process. The resultant saline aqueous phase was transferred to the extraction tank at the start of the next extraction batch.

3.4. Toluene tests: measurements of k_f^{shell}

Liquid film mass transfer coefficients in the membrane lumen can be estimated using correlations, such as the L ev eque correlation. However, evaluation of the shell side liquid film mass transfer resistance using purely mathematical tools is rather difficult. Therefore, a separate experimental study for estimation of shell side liquid film mass transfer coefficients was performed at different temperatures, mixing residence times, and scales. The experimental strategy for k_f estimation is to measure the overall mass transfer coefficient in a scenario, where the mass transfer liquid film resistance outside the membrane tube is the main resistance.

Toluene was chosen as the model compound for liquid film mass transfer coefficient measurements. Toluene has a similar molecular structure and size to that of phenol but does not have any acid–base functionality. Furthermore, the diffusion coefficients in water at 30°C for toluene ($1.1 \times 10^{-9} \text{ m}^2 \text{ s}^{-1}$) and phenol ($1.0 \times 10^{-9} \text{ m}^2 \text{ s}^{-1}$) calculated by the Wilke–Chang correlation [8] are similar, but toluene has much higher volatility and permeability through the silicone rubber membrane, making it an ideal candidate for liquid film resistance estimation. The high permeability through silicone rubber membrane ensures a toluene membrane mass transfer coefficient in the range of 10^{-5} m s^{-1} [9,10], which makes the liquid film the dominant mass transfer resistance. Vapour pressures at 50°C for phenol and toluene are, respectively, 2.6 and 91.4 mmHg [8]. The high toluene volatility guarantees that it can easily be stripped into a gas phase, where the gas film resistance is negligible. Therefore, the Eq. (1), with three resistances in series, simplifies into Eq. (2). An air flow of 3 L min^{-1} inside the membrane tubes, ensured simultaneously that k_s and $A_{s,b}$ are negligible

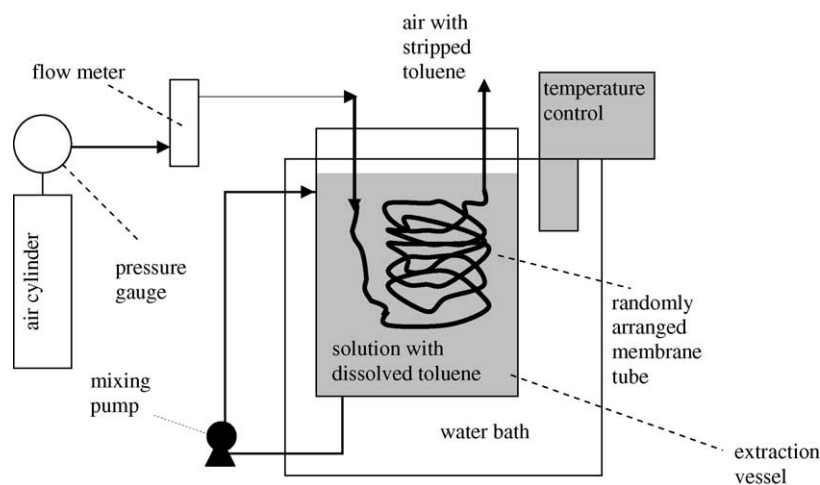


Fig. 6. Schematic diagram of experimental set-up for k_f^{shell} measurements at lab scale.

and that Eq. (5) (with $A_{f,b}$ as bulk toluene concentrations at the membrane shell side) can be used to estimate the overall toluene mass transfer coefficients.

The liquid film mass transfer coefficient is usually defined as a ratio of the diffusion coefficient of the transported specie to the stagnant liquid film thickness. Therefore, since phenol and toluene have similar diffusion coefficients, this study assumes that the phenol liquid film mass transfer coefficients are similar to the ones measured for toluene at the same operating conditions (membrane module, shell side mixing rates, temperature and solution viscosity).

Fig. 6 illustrates the laboratory experimental set-up for estimation of the membrane shell side liquid film mass transfer coefficient, k_f^{shell} . An aqueous toluene solution was recirculated through the membrane shell side, while an air flow of 3 L min^{-1} was fed in one pass through in the membrane lumen. Samples were taken periodically from the extraction tank. The experiments were performed varying different parameters, such as temperature, feed solution residence time and membrane length. Further details will be presented in Section 4.

For estimation of the scaling up effects on the shell side liquid film mass transfer coefficient, similar experiments were performed in the pilot plant unit (Fig. 4) as well. The toluene tests were carried out as follows: the extraction tank was filled with an aqueous solution of toluene, the stripping solution was discharged from the membrane lumen into the stripping solution tank and replaced with a constant air flow (Fig. 4). Pump 1 mixing rate was kept the same as during the phenol extraction, which corresponds to a liquid residence time of 11 min. Samples from the extraction tank were taken every 20 min. Both membrane modules used for phenol extraction (Fig. 5) were tested in the same manner.

4. Results and discussion

4.1. Overview of the MARS performance

Extraction and recovery efficiencies are shown in Fig. 7. An average value for phenol extraction efficiency of 94% was estimated for batches 3–15 with a coefficient of variation of 4%. In these batches, the phenol content in the wastewater outlet discharged after MARS detoxification was lower than 0.37 wt.%. Such phenol concentrations are low enough that the wastewater can be submitted for further detoxification by a suitable destructive process (Fig. 2) [11].

Reagent (NaOH and HCl) consumption during the extraction and recovery stages followed chemical reaction stoichiometric requirements, except for batches 7–11 where a leak was found in the membrane between the wastewater and the stripping solution phases. Phenol mass balances over the extraction and the recovery stages closed for all 15 batches. With the exception of the first four batches, the overall MARS phenol mass balance also closed. It was found that the higher the HCl concentration added to the recovery stage, the more

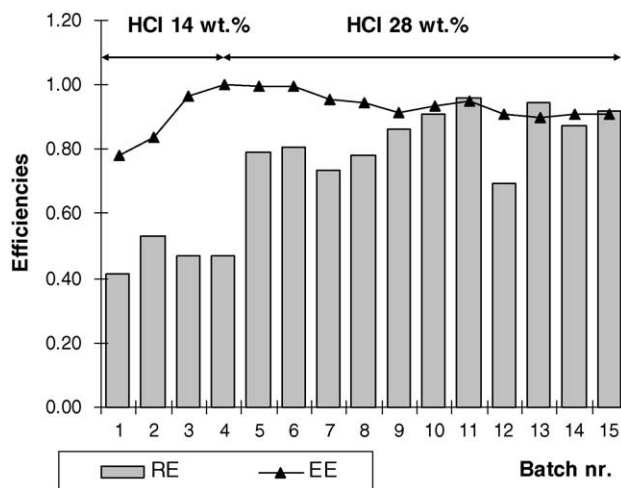


Fig. 7. Extraction (EE) and recovery (RE) efficiencies for the 15 batches.

efficient the MARS performance was, increasing both the recovery efficiency and decreasing the saline layer (SLR) and dilution ratios (SDR and PDR).

Average recovery efficiency was 84%, with 11% coefficient of variation, for batches 5–15. The recovered “wet” phenol, with 20–23 wt.% water contents was successfully reused in the resin production process, suggesting that integration of MARS into a resin plant site is feasible and can avoid off-site phenolic wastewater disposal.

4.2. Effect of the stripping solution pH on the extraction efficiency and on the wastewater outlet phenol concentrations

The extraction efficiency (EE) is related to phenol mass transfer through the membrane as expressed by Eq. (6). The extraction efficiencies shown in Fig. 7 are fairly constant over batches 3–15 as is the phenol concentration (Fig. 8) in

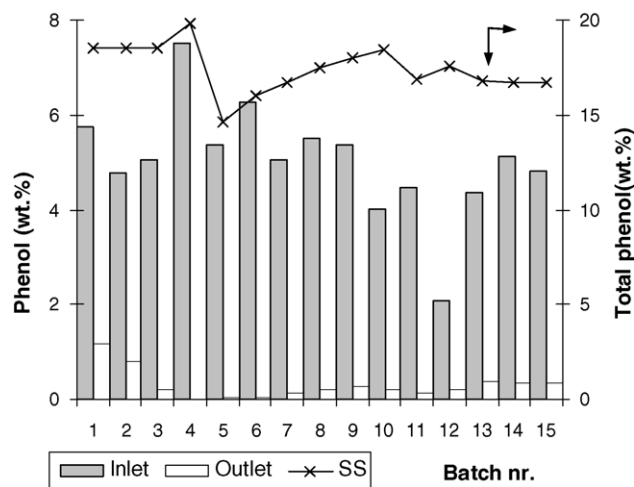


Fig. 8. Inlet, outlet and stripping solution phenol concentrations for the 15 batches.

the wastewater outlet, discharged from the MARS extraction tank.

The extraction efficiencies for batches 1 and 2 were substantially lower than the subsequent batches (around 80%), and the respective wastewater outlet concentrations are higher. This result was attributed to the fact that the first two batches were performed at a stripping solution pH around 11.5, while for the following batches this pH value was increased to values between 12.8 and 13.2. Moreover, batch 1 was performed at 30 °C, and, since the membrane permeability decreases with temperature [1], the lowest extraction efficiency was observed.

The total phenol concentration measured in the stripping solution ($C_{s,b}^T$) over the 15 batches, shown in Fig. 8, corresponds to an average value of 17.4 wt.% with a coefficient of variation of 7.3%. This experimental value is lower than the theoretical value for total phenol at steady state of 19.9 wt.%, calculated by Eq. (12) for a stripping solution controlled at steady state via addition of 10.4 wt.% NaOH [6]. In spite of a drop in its value from batches 4–5, the total phenol concentration in the stripping solution is fairly constant over the 15 batches and it can be assumed that is at steady state.

$$C_{s,b}^T (\text{wt.}\%) = \frac{100}{1 + (\text{Mw}_{\text{NaOH}}/\text{Mw}_{\text{PhOH}})(100/C_{\text{NaOH}}^{\text{Add}} (\text{wt.}\%))} \quad (12)$$

The pH effect can be explained as following. Phenol concentration in the wastewater extraction tank solution ($A_{f,b}$) decreases over time as the batch progresses, and by the end of the batch, the concentration of neutral phenol in the stripping solution ($A_{s,b}$), eventually becomes comparable to $A_{f,b}$, thus, reducing the mass transfer rate (Eq. (3)). On the other hand, as the stripping solution pH decreases, $A_{s,b}$ increases (Eq. (13)) [1], resulting again in a lower driving force for the phenol mass transfer through the membrane (Eq. (3)).

$$A_{s,b} = \frac{C_{s,b}^T}{1 + 10^{\text{pH} - \text{p}K_a}} \quad (13)$$

The calculated total phenol concentration (Eq. (12)), $C_{s,b}^T = 19.9$ wt.%, and the $\text{p}K_a$ of 10 for phenol were used to calculate the neutral phenol concentration ($A_{s,b}$), from Eq. (13). The corresponding $A_{s,b}$ value for the stripping solution pH 12.8–13.2 is 0.03–0.01 wt.%, whereas for pH 11.5, this value is one order of magnitude higher, 0.58 wt.%. Therefore, for the first two batches, operated at pH 11.5, $A_{s,b}$ had a major and earlier impact on the phenol extraction driving force, leading to the lower extraction efficiencies and higher wastewater outlet phenol concentrations observed.

For the overall phenol mass transfer coefficient calculation, Eq. (5) assumes that $A_{s,b}$ is negligible for the driving force (i.e. $A_{f,b} - A_{s,b} \approx A_{f,b}$). This assumption holds for the first hours of the extraction batch, but as the feed solution concentration decreases towards the end of the batch it can lose its accuracy, which translates into a loss of linearity of Eq. (5). The overall mass transfer coefficients were estimated

using exclusively measurements from the linear region (taking into account only points with coefficient of linear correlation not less than 0.995), thus the phenol concentration values at the end of extraction batches 8–11 have been neglected.

4.3. HCl concentration effects on MARS process

4.3.1. Recovery stage: recovery efficiency and saline layer ratio

The phenol recovery efficiency is a measure of how much of the extracted phenol is fed back into the resin production process. Recovery efficiencies are shown in Fig. 7 and, in spite of the scattering of the data, it is noticeable that the higher HCl concentration used for neutralization in the recovery stage led to higher recovery efficiency. NaOH concentration added to the stripping solution was kept at a constant value of 10.4 wt.% for the entire MARS trial. However the HCl concentration used in the recovery stage was doubled from 14 to 28 wt.%, resulting in an increase of the average recovery efficiency from 47 to 84%, with corresponding coefficients of variation of 9.9 and 10.5%.

When higher amounts of water are introduced into the MARS process through the HCl solution (14 wt.% versus 28 wt.%), so a larger volume of aqueous saline layer is generated, and hence, a lower NaCl concentration is present in the aqueous layer (calculated values 7.7 wt.% versus 11.2 wt.%). This reduces the salting out effect, and results in higher phenol concentrations in the aqueous layer (4.2 wt.% versus 3.4 wt.% [1]), lower masses of the generated wet organic rich layer, and lower recovery efficiencies, respectively. This effect is quantified by the saline layer ratio (SLR) defined in the process performance analysis section and shown in Fig. 9.

Therefore, the higher the HCl concentration employed in the recovery stage, the better the MARS performance should be, with higher recovery efficiencies and lower saline layer ratio. However, the HCl concentrations used in the MARS recovery stage are limited by safety precautions related to the partial vapour pressure of HCl. For example, at 30 °C, the 14

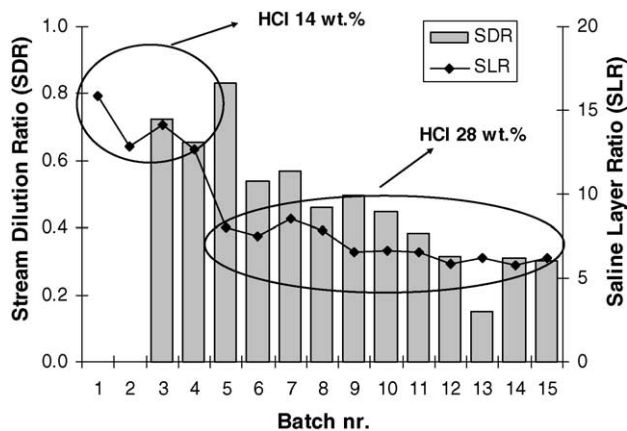


Fig. 9. Saline layer ratio (SLR) and stream dilution ratio (SDR) for the 15 batches.

and 28% HCl aqueous solutions employed in this study have partial pressures of, respectively, 6×10^{-5} and 0.013 atm, while at concentrations of 34 and 38% (commercially available) the respective HCl partial pressures are already 0.24 and 0.47 atm.

The recovery efficiencies and the saline layer ratio are also affected by the concentration of NaOH added to the stripping solution in the extraction stage. As shown in Eq. (12), the higher the NaOH concentration ($C_{\text{NaOH}}^{\text{Add}}$) the higher the total phenol ($C_{\text{s,b}}^{\text{T}}$), and sodium phenolate concentrations in the stripping solution at steady state. As a result, higher NaCl concentrations are generated in the aqueous phase at the recovery stage, thus enhancing the salting out effect and achieving higher MARS recovery efficiencies. However, the higher the total phenol concentration ($C_{\text{s,b}}^{\text{T}}$), the higher the stripping solution viscosity and, for a given pH, the higher the neutral phenol concentration ($A_{\text{s,b}}$) (Eq. (13)). A higher neutral phenol concentration in the stripping solution ($A_{\text{s,b}}$) reduces the driving force for mass transfer and a higher stripping solution viscosity increases the stripping solution liquid film resistance to mass transfer.

4.3.2. Dilution ratios

At the end of each recovery, the aqueous saline phase is recirculated to the extraction tank, implying that the actual volume of feed solution submitted to the extraction stage is larger than the industrial resin wastewater inlet, and that additional phenol has to be reextracted through the membrane. The stream dilution ratio (SDR) is a measure of the reduction in fresh wastewater volume treated by the MARS process due to the recirculation of the saline aqueous layer (i.e. a net increase in wastewater that has to be treated by the MARS extraction stage). For a fixed extraction tank volume, the higher the SDR, the lower is the volume of resin plant wastewater treated during each MARS batch. In other words, detoxification of a certain wastewater volume at higher SDR, for a given extraction tank volume and extraction efficiency, requires either (i) a higher number of batches or (ii) the same number of batches, but performed using higher membrane areas.

The experimental stream dilution ratios (SDR) are shown in Fig. 9, and illustrate that once the concentration of HCl used was increased from 14 to 28 wt.%, SDR values decreased from an average value of 0.7–0.4. Thus, in the later batches (with 28 wt.% HCl) 60% of the mass fed to MARS extraction was actually derived from the resin wastewater plant, instead of the lower value of 30% obtained when 14 wt.% HCl was used.

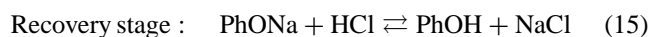
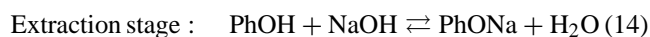
The phenol dilution ratio (PDR) is a measure of how much of the phenol fed to extraction is carried by the aqueous saline layer, and therefore, how much extra phenol has to be reextracted through the membrane due to the aqueous saline layer recirculation. PDR decreased from an average value of 0.5–0.2 (standard deviation of 0.1), indicating that 80% of the membrane is actually used to extract phenol derived from

the resin wastewater stream, while in the previous case 50% of the membrane area was extracting phenol from the MARS recovery stage.

The effect of HCl concentration is not as distinctive in the stream dilution ratio (SDR) as in the saline layer ratio (SLR) (Fig. 9), because the first two batches were performed without recirculation of the aqueous saline layer to the extraction stage, and the accumulated saline layer was recirculated into extraction batch 3. Moreover, a dilution ratio steady state value can be reached after a certain number of batch operations for each of the HCl concentration values.

4.4. Reagent ratios and membrane leakage

The acid base reactions that take place in the stripping solution and at the recovery stage are equimolar reactions:



Reactions (14) and (15) theoretically correspond to molar extraction (NaOH/Phenol) and recovery ratios (HCl/phenol) of unity, respectively. The experimental extraction ratios shown in Fig. 10 are usually higher than 1.0 due to the extra NaOH required to maintain the stripping solution pH at an alkaline value. The recovery ratios are also usually higher than 1.0 because of the extra HCl added to ensure that all the phenol is in the neutral form at a pH lower than 3.

The recovery ratios are about 1.0 for all the batches, and the extraction ratios are near unity for batches 1–6 and 12–15. In batches 7–11, a leakage in the membrane was identified, allowing acidic feed solution to pass into the alkaline stripping solution. Consequently, the moles of NaOH added to keep the stripping solution pH constant were nearly twice the chemical reaction stoichiometric requirement, as can be seen from the extraction ratio for these batches (Fig. 10). In these batches, the feedback loop maintaining the feed solution pH lower than 3 was activated, indicating leakage of

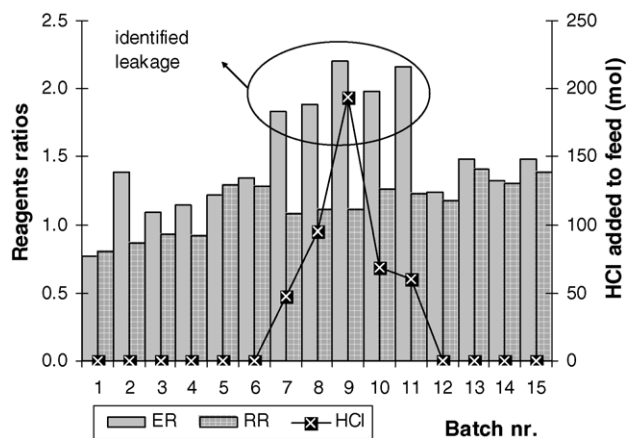


Fig. 10. Extraction ratio (ER), recovery ratio (RR) and moles of HCl added to the wastewater extraction tank for the 15 batches.

the alkaline stripping solution into the extraction tank. The amount of HCl added to the extraction tank to neutralize the leakage is also shown in Fig. 10. After batch 11, the damaged membrane module I was replaced by module II and during the following batches the extraction ratio was restored to values near unity.

4.5. Mass balances and final product purity

Three phenol mass balances have been defined for the MARS process, indicated with dashed line boxes in Fig. 1. The first mass balance (Eq. (16)) was struck for the extraction stage and compares the phenol in the stripping solution overflow (“SS” in Fig. 1) with the phenol extracted from the feed solution, that is the difference between the amount of phenol fed (“Feed” in Fig. 1) to the extraction stage and the phenol in the extraction outlet stream (“Outlet” in Fig. 1). This mass balance assumes a steady state concentration for the solution in the stripping tank. The cumulative mass balance (over the 15 batches) for the extraction stage was closed within 4.2%. The second phenol mass balance for the recovery stage (Eq. (17)) compares the amount of phenol in the stripping solution overflow fed to recovery (“SS” in Fig. 1) with the phenol in the two phases generated after neutralization: the wet organic phase (“Org” in Fig. 1) and the saline aqueous layer (“Aq” in Fig. 1). The cumulative mass balance (over the 15 batches) for the recovery stage was closed within 1.1%.

$$\begin{aligned} \text{Phenol (kg) in SS} &= \text{Phenol (kg) in Feed} \\ &\quad - \text{Phenol (kg) in Outlet} \end{aligned} \quad (16)$$

$$\begin{aligned} \text{Phenol (kg) in SS} &= \text{Phenol (kg) in Org} \\ &\quad + \text{Phenol (kg) in Aq} \end{aligned} \quad (17)$$

An overall process mass balance for the MARS process was done by comparing the phenol amount in the resin wastewater condensate (“Inlet” in Fig. 1) and the outlet streams. The outlet streams comprise the wastewater discharged from extraction tank (“Outlet” in Fig. 1) plus the recovered phenol in the wet organic phase (“Org” in Fig. 1).

$$\begin{aligned} \text{Phenol (kg) in Inlet} &= \text{Phenol (kg) in Org} \\ &\quad + \text{Phenol (kg) in Outlet} \end{aligned} \quad (18)$$

The cumulative mass balance for phenol (over the whole 15 batches) for the overall MARS process is shown in Fig. 11. It indicates losses of about 52 kg phenol, which represents about 13.8% of the total 376 kg phenol in the resins wastewater (“Inlet” stream) fed to the MARS unit. However, the greatest part of the phenol losses appeared in the first four batches and after batch 5 the mass balance was closed within 3%. This result can be attributed to the following: (i) the stripping solution concentration oscillation between batches 4 and 5 (Fig. 8), (ii) the appearance of a small amount of organic-aqueous emulsion phase in the separation step, which is not recirculated back into the MARS process, and hence, is not

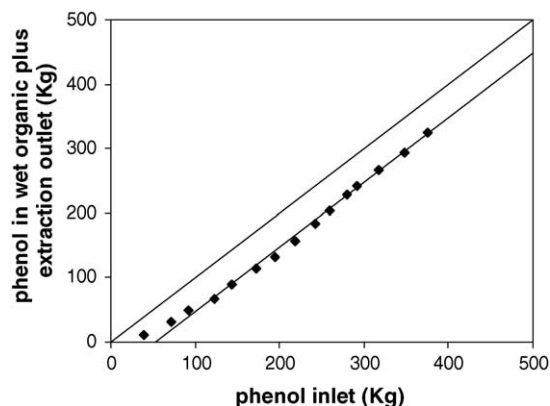


Fig. 11. Overall process phenol mass balance.

accounted for in the mass balance, and (iii) phenol accumulation in the system until a steady state is achieved, especially for the first three batches with an atypical aqueous phase recirculation.

Fig. 12 shows the composition of the phenol rich organic layer, which has an average content of 78.8 ± 4.6 wt.% phenol and 20.4 ± 2.1 wt.% water. This phenol rich organic layer was fed back to the original manufacturing process and successfully used as a reagent for resin production.

4.6. Mass transfer studies

4.6.1. Liquid film feed solution mass transfer coefficients

The membrane permeability for toluene through silicone rubber at 30 and 50 °C has been measured elsewhere as $2.2 \times 10^{-8} \text{ m}^2 \text{ s}^{-1}$ [9] (or $2.6 \times 10^{-8} \text{ m}^2 \text{ s}^{-1}$ [10]) and $5.2 \times 10^{-8} \text{ m}^2 \text{ s}^{-1}$ [9]. For the membrane tube dimensions used, such values correspond to a membrane mass transfer coefficient (k_m) of $5.0 \times 10^{-5} \text{ m s}^{-1}$ and $7.2 \times 10^{-5} \text{ m s}^{-1}$, respectively, at 30 and 50 °C. As already mentioned, the vapour pressure of toluene is quite high and toluene is easily extracted from a liquid phase, through the membrane and stripped into a gas phase. The overall toluene mass transfer coefficient values were estimated by Eq. (5) as the average of three

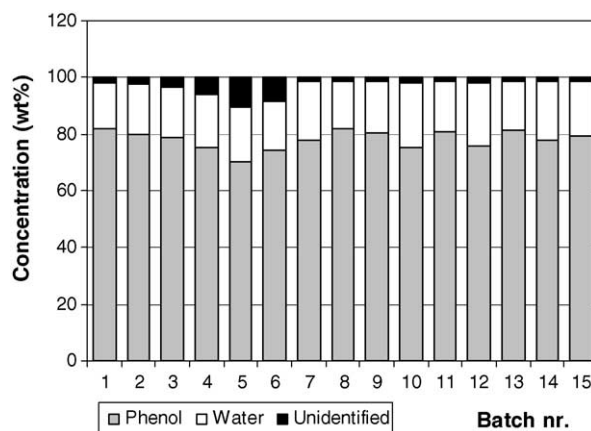


Fig. 12. Recovered phase composition.

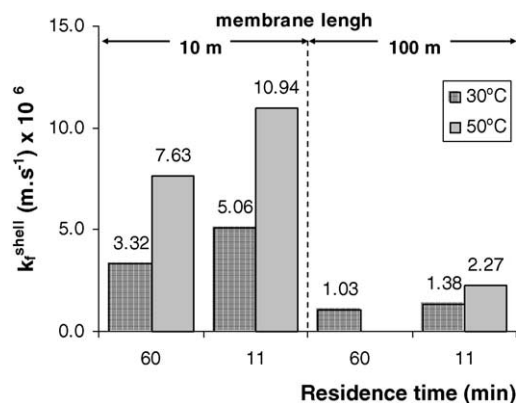


Fig. 13. Feed shell side liquid film mass transfer coefficient (k_f^{shell}) measured at lab scale in a 5 L vessel.

independent measurements, with coefficients of variation lower than 10%. The feed liquid film mass transfer coefficients at the membrane shell side (k_f^{shell}) shown in Figs. 13 and 14 were calculated from Eq. (2), using the measured overall toluene mass transfer coefficients, and k_m based on the membrane permeability literature values at the respective temperatures.

k_f^{shell} was estimated at lab scale (Fig. 13) for (i) two different temperatures, 30 and 50 °C, (ii) two different membrane lengths, 10 and 100 m, and (iii) two different hydrodynamic conditions, corresponding to different pump mixing rates and expressed as two different residence times, 11 and 60 min, for the 4 L of feed solution in the 5 L extraction vessel. Fig. 13 shows that k_f^{shell} increases as temperature increases. This effect is associated with the effect of temperature on the aqueous toluene diffusion coefficient. The Wilke–Chang correlation predicts an increase in toluene diffusion coefficient of about 1.7 times, as temperature increases from 30 to 50 °C. This value is within the ratios of experimentally estimated k_f^{shell} values at these two different temperatures (1.6–2.3).

As the residence time increases from 11 to 60 min at lab scale (5 L vessel), an increase in the experimentally

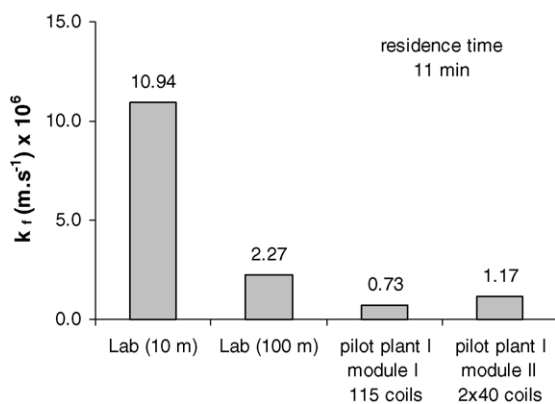


Fig. 14. Effect of scaling up on the feed shell side liquid film mass transfer coefficient (k_f^{shell}).

estimated k_f^{shell} value of about 1.3–1.5 times is observed. It is difficult to define a Reynolds number for the feed solution at the membrane shell side, but an increase in feed recirculation residence time, implies worsening the hydrodynamic conditions at the membrane shell side, and therefore, an increase in the theoretical liquid film thickness.

It was observed that the mass transfer decreases as the membrane length increases. In all the lab experiments, 4 L of feed solution (5 L vessel) was used, and thereby, increasing the membrane area 10 times, from 10 to 100 m length, implies that the membrane tube becomes more closely packed inside the 5 L extraction vessel. This can lead to stagnant volumes of solution and poor mixing of the feed solution. Interpretation of such phenomena using the liquid film theory can be translated as an increase in liquid film thickness.

For the toluene test in the pilot plant unit, a residence time of 11 min and a temperature of 50 °C were used. The membrane mass transfer coefficient (k_m) for toluene was still taken into account in the k_f^{shell} calculations, although its value is negligible compared to the estimated k_f^{shell} values. Thus, it can be assumed that the feed solution liquid film resistance at the membrane shell side is actually the only significant mass transfer resistance. The scaling up effect on k_f^{shell} is shown in Fig. 14, which illustrates that increasing the membrane tube length or the number of membrane coils in one-compartment results in k_f^{shell} reduction. Therefore, as the process is scaled up, it becomes more difficult for good mixing of the feed solution to be achieved, most probably due to constrictions of the membrane tubes inside the extraction tank and poor fluid circulation. The module II configuration (Fig. 5) is obviously more successful and demonstrates improved mass transfer performance.

4.6.2. Overall mass transfer coefficients at pilot scale, experimental and theoretical

Eq. (5) was used to estimate overall phenol mass transfer coefficients at pilot scale. This equation assumes that the back concentration of neutral phenol ($A_{s,b}$) in the stripping solution is negligible in the driving force and in comparison with the feed solution phenol concentrations ($A_{f,b}$). As discussed before, this assumption is not valid for batches 1 and 2 performed at pH 11.5, and therefore, these batches have been discarded from the mass transfer analyses. A leak between the feed and the stripping solution was identified for batches 7–11, and therefore, the mass transfer coefficients estimated for these batches were also discarded. The experimentally obtained overall phenol mass transfer coefficients (K_{ov}) values for module I (batches 3–6) and for module II (batches 12–15) are presented in Fig. 15. The average for the batches mass transfer coefficient value in module I is $(1.48 \pm 0.14) \times 10^{-7} \text{ m s}^{-1}$, while in module II is $(1.73 \pm 0.04) \times 10^{-7} \text{ m s}^{-1}$. This result is logical, since as illustrated in Fig. 5, module II has a more open structure and an improved mixing of the feed solution is expected for this configuration.

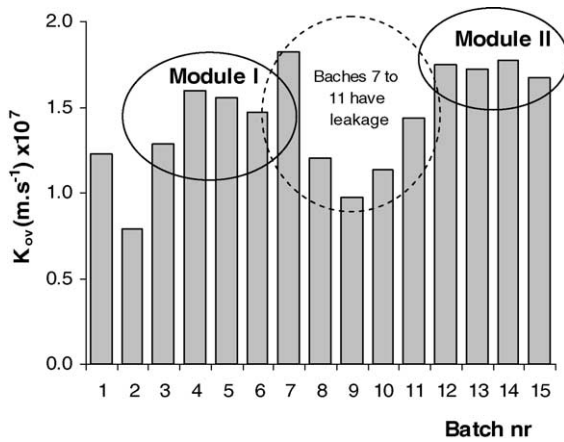


Fig. 15. Overall mass transfer coefficients for the 15 batches.

It is interesting now to compare these experimental overall mass transfer coefficient values with the theoretically estimated ones. The theoretical values were calculated from Eq. (5) using the k_m value of $2 \times 10^{-7} \text{ m s}^{-1}$ [7] and the feed solution liquid film mass transfer coefficients (k_f^{shell}), estimated from the toluene test for each module. The theoretical and the experimental values, presented in Table 2, are in a good agreement showing that the differences in the overall phenol mass transfer results, observed for the pilot unit, can be explained on the basis of the feed solution liquid film resistance at the shell side of the randomly coiled membrane.

The overall mass transfer coefficient calculations were done assuming that $A_{s,b}$ is negligible in the mass transfer driving force, and that the stripping solution is homogeneous along the membrane tube lumen. The accuracy of these assumptions for the operating stripping solution pH (12.8–13.2) depends on the flow rate of the recirculated stripping solution. At too low flow rates, axial phenol concentration and pH gradients occur in the membrane tube. A too high flow rate can result in a high pressure drop alongside the membrane, which may exceed the membrane tube burst pressure. For a tube of 100 m, length and the operating conditions used, a flow rate of $1.5 \text{ dm}^3 \text{ h}^{-1}$ per membrane tube ensures the stripping solution homogeneity and is far from the burst pressure limit [12].

Table 2
Comparison between the theoretical and the experimental overall mass transfer coefficients

Module	Mass transfer coefficient $\times 10^7 \text{ m s}^{-1}$		
	Exp. k_f^{shell}	Calc. K_{ov}	Exp. K_{ov}
I	7.27	1.57	1.48
II	11.69	1.71	1.73

Calc. K_{ov} based on exp. k_f^{shell} and $k_m = 2.0 \times 10^{-7} \text{ m s}^{-1}$.

5. Conclusions

In this study, a MARS process pilot plant was successfully introduced to a phenolic resin production plant site. The MARS unit was able to recover phenol from the plant wastewater with phenol contents between 2 and 8 wt.%. An average phenol extraction efficiency of 94% was achieved. The results obtained show the potential application of MARS technology as a process able to reduce the phenol concentrations to a values sufficiently low (e.g. 0.1–0.3 wt.%) for further phenol detoxification by destructive processes, such as biodegradation or chemical oxidation.

The integration of the MARS process in a resin plant site avoids the off-site phenolic wastewater disposal and benefits by the additional phenol recovered. The average phenol recovery efficiency was 84%. The recovered “wet” phenol with 20–23 wt.% water contents was successfully reused in the resin production process.

The influence of the aqueous saline layer recirculation on the overall process performance was evaluated. The results showed that if HCl solution with higher concentration is used at the recovery stage lower stream dilutions are obtained. For example, when the HCl concentration was increased from 14 to 28 wt.% the stream dilution ratio descended from 0.7 to 0.4, and the recovery efficiency increased from 46 to 84%.

The effect of scaling up on phenol mass transfer for a MARS batch configuration was studied in this paper and was concluded that the differences in the overall phenol mass transfer coefficients are mainly due to the feed solution liquid film resistance at the membrane shell side. Therefore, the mass transfer rates can be improved by intensifying mixing at the membrane shell side.

Although the only “waste” generated from the MARS technology is NaCl, which makes this process “greener” than most of its competitive technologies further improvement in that direction could be made. For example, an electro dialysis unit could be included for partial regeneration of NaCl in the saline aqueous layer with production of NaOH and HCl as an additional benefit to the process. Another possible direction for the MARS process intensification could be implication of different membrane material possessing better mass transfer properties (higher phenol permeability) and extended operational lifetime under extreme alkaline conditions.

Acknowledgements

This work was funded by the U.K. Engineering and Physical Sciences Research Council (EPSRC) Grant GR/R57188/01. F.C. Ferreira acknowledges financial support from Fundação para a Ciência e Tecnologia, Grant PRAXIS XXI/BD/21448/99.

Appendix A. Maximum mass transfer enhancement by chemical reaction: simplification of Eq. (1) into Eq. (2)

Eq. (2) assumes that the stripping solution liquid film resistance is negligible. In other words, that the enhancement factor (E) has a value high enough to completely eliminate the stripping solution liquid film resistance term $1/Ek_s$ into Eq. (1). We have based this assumption on the following calculations:

According to the Olander model [6] (for a second order reversible chemical reaction) the enhancement factor in the MARS process can be expressed by Eq. (1A):

$$E = 1 + \frac{D_{\text{PhO}^-}}{D_{\text{PhOH}}} \frac{KB_{s,b}}{1 + (D_{\text{PhO}^-}/D_{\text{OH}^-})KA_{s,i}} \quad (1A)$$

Diffusion coefficients for phenol (D_{PhOH}), hydroxide (D_{OH^-}) and phenolate (D_{PhO^-}) can be found in the literature [13] and the equilibrium constant ($K = 10^4 \text{ M}^{-1}$) can be obtained from the literature value for the phenol dissociation acid constant ($K_a = 10^{-10} \text{ M}$). Following the analytical solution presented by authors elsewhere [6] the phenol concentration at the interface between the membrane and the stripping solution ($A_{s,i}$) can be calculated by Eq. (2A).

$$A_{s,i} = \frac{-b + \sqrt{b^2 - 4ac}}{2a} \quad (2A)$$

where,

$$a = \left(1 + \frac{k_g}{k_s}\right) \frac{D_{\text{PhO}^-}}{D_{\text{OH}^-}} K$$

$$b = \left(1 + \frac{k_g}{k_s}\right) + \frac{D_{\text{PhO}^-}}{D_{\text{PhOH}}} KB_{s,b} - \left(A_{s,b} + \frac{k_g}{k_s} A_{f,b}\right) \frac{D_{\text{PhO}^-}}{D_{\text{OH}^-}} K$$

$$c = - \left[\frac{k_g}{k_s} A_{f,b} + A_{s,b} \left(1 + \frac{D_{\text{PhO}^-}}{D_{\text{PhOH}}} KB_{s,b}\right) \right]$$

All parameters employed in the foregoing calculations are summarised in Table A.1 and described below:

- $A_{f,b}$: As shown in Fig. 8, the phenol feed concentrations ($A_{f,b}$) varies between 8 and 0.1 wt.% (0.851 and 0.001 M), and therefore, the enhancement factor was calculated for each of these concentrations.
- $B_{s,b}$: The stripping solution was maintained at a stripping solution pH of 12.8, which corresponds to a hydroxide concentration ($B_{s,b}$) of 0.063 M.
- $A_{s,b}$: The total phenol in the stripping solution was maintained at a fairly constant value of 17.4% (1.85 M) during

the process. However, for the enhancement factor calculations the theoretically estimated by Eq. (12) value of 19.9 wt.% (2.12 M) was used. The latest total phenol concentration corresponds to a neutral phenol concentration ($A_{s,b}$) of 0.03 wt.% in the stripping solution (pH 12.8) according to Eq. (13).

- k_m : Membrane mass transfer coefficient (k_m) for phenol of $2 \times 10^{-7} \text{ m s}^{-1}$ [7].
- k_f : Liquid film mass transfer coefficient for the feed solution at the membrane shell side. k_f of $1 \times 10^{-6} \text{ m s}^{-1}$ was used for the calculations. This value is within the estimated range of k_f in this study.
- k_s : The liquid film mass transfer coefficients in the membrane tube lumen (k_s) can be estimated from the Lévêque correlation for laminar regimes. Although previous works [14,15] suggested that this correlation slightly underestimates the mass transfer coefficients, the Lévêque correlation was still used to determine the range of k_s . As long as the purpose of this calculation is to estimate rather the range of the stripping solution liquid film resistance term $1/Ek_s$ then its actual value this approach will not introduce significant error in the calculations. Thus, k_s was estimated at a value of $8.5 \times 10^{-7} \text{ m s}^{-1}$ using Lévêque correlation for a stripping solution with a density of 1.1 kg L^{-1} and viscosity of 1.9 cP flowing inside a membrane tube with an internal radius of 1.5 mm at a flow rate of 1.5 L h^{-1} .

Enhancement factors of 56 and 99 were calculated, respectively, for $A_{f,b}$ of 8 and 0.1 wt.% using Eqs. (1A) and (2A) and employing the parameters summarized in Table A.1. Substituting each of these E values and the mass transfer coefficients in Eq. (1), the calculated overall mass transfer coefficient differs only within 1% from the one calculated by Eq. (2), and therefore, it was concluded that Eq. (2) can be applied accurately for the operating conditions employed and the stripping solution liquid film resistance neglected in the calculations.

Nomenclature

$A_{f,b}$	phenol (or toluene) concentration in the bulk of the feed solution at the shell side of the membrane tubes (wt.%)
$A_{s,b}$	neutral phenol concentration in the bulk of the stripping solution (wt.%)
Aq	in the saline aqueous phase (Fig. 1)
$C_{\text{NaOH}}^{\text{add}}$	concentration of NaOH added to the stripping solution (wt.%)
$C_{s,b}^T$	total phenol concentration in the bulk of the stripping solution (wt.%)
E	enhancement factor for mass transfer due to chemical reaction
EE	extraction efficiency
Ext	phenol extracted through the membrane (Fig. 1)
Feed	in the feed solution to the extraction tank (Fig. 1)
H_2O	water
H_3O^+	hydronium ion
Inlet	resin wastewater condensate inlet stream (Fig. 1)

Table A.1

Resume of parameters for appendix calculations

$D_{\text{PhOH}} = 0.89 \times 10^{-9} \text{ m s}^{-2}$	$A_{f,b} = 8 \text{ and } 0.1 \text{ wt.}\%$
$D_{\text{PhO}^-} = 0.86 \times 10^{-9} \text{ m s}^{-2}$	$A_{s,b} = 0.03 \text{ wt.}\%$
$D_{\text{OH}^-} = 5.3 \times 10^{-9} \text{ m s}^{-2}$	$B_{s,b} = 0.063 \text{ M (pH 12.8)}$
$K = 10^4 \text{ M}^{-1}$ ($\text{p}K_a = 10$)	$k_m = 2 \times 10^{-7} \text{ m s}^{-1}$
$\text{MW}_{\text{PhOH}} = 94 \text{ g mol}^{-1}$	$k_f = 10 \times 10^{-7} \text{ m s}^{-1}$
$\text{MW}_{\text{NaOH}} = 40 \text{ g mol}^{-1}$	$k_s = 8.5 \times 10^{-7} \text{ m s}^{-1}$

k_f	liquid film mass transfer coefficient in the feed solution (m s^{-1})
k_f^{shell}	liquid film mass transfer coefficient in the feed solution at the membrane shell side (m s^{-1})
k_g	grouped mass transfer coefficient (m s^{-1})
k_m	membrane mass transfer coefficient (m s^{-1})
k_s	liquid film mass transfer coefficient in the stripping solution at the membrane tube lumen (m s^{-1})
K_a	acid base dissociation constant for phenol (M)
K_{ov}	overall mass transfer coefficient (m s^{-1})
MW_{NaOH}	molecular weight of sodium hydroxide (kg kmol^{-1})
MW_{PhOH}	molecular weight of phenol (kg kmol^{-1})
NaCl	sodium chloride
NaOH	sodium hydroxide
Org	in the organic phase (Fig. 1)
Out	in the feed solution discharged from MARS extraction after detoxification (Fig. 1)
pH	$-\log \text{H}_3\text{O}^+$
$\text{p}K_a$	$-\log K_a$
P	membrane permeability ($\text{m}^2 \text{s}^{-1}$)
PDR	phenol dilution ratio
PhOH	phenol
PhONa	sodium phenolate
r_i	membrane tube internal radius (m)
r_o	membrane tube external radius (m)
RE	recovery efficiency
S_m	membrane area (m^2)
SDR	stream dilution ratio
SLR	saline layer ratio
SS	in the stripping solution overflow from the extraction stage and fed to the recovery stage (Fig. 1)
t	time (s)
V_f	volume of feed solution in the extraction tank (m^3)

References

- [1] S. Han, F. Castelo Alves Ferreira, A.G. Livingston, Membrane Aromatic Recovery System (MARS)—a new membrane process for the recovery of phenols from wastewaters, *J. Membr. Sci.* 188 (2) (2001) 219–233.
- [2] F. Castelo Alves Ferreira, S. Han, A.G. Livingston, Recovery of aniline from aqueous solution using the Membrane Aromatic Recovery System (MARS), *Ind. Eng. Chem. Res.* 41 (2002) 2766–2774.
- [3] F. Castelo Alves Ferreira, S. Han, A.T. Boam, S. Zhang, A.G. Livingston, Membrane Aromatic Recovery System (MARS): lab bench to industrial pilot scale, *Desalination* 148 (2002) 267–273.
- [4] EPA: US Environmental Protection Agency, EPA: List of Priority Pollutants, 2003.
- [5] S. Bizzari, Chemical Economics Handbook Report, Phenol, SRI Chemical and Health Business Services, 2002.
- [6] F. Castelo Alves Ferreira, L.G. Peeva, A.G. Livingston, Mass transfer enhancement in the Membrane Aromatic Recovery System (MARS): theoretical analysis, *Chem. Eng. Sci.* 60 (2005) 151–166.
- [7] F. Castelo Alves Ferreira, L.G. Peeva, A.G. Livingston, Mass transfer enhancement in the Membrane Aromatic Recovery System (MARS): experimental results and comparison with theory, *Chem. Eng. Sci.* 60 (2005) 1029–1042.
- [8] R.H. Perry, D.W. Green, *Perry's Chemical Engineers' Handbook*, seventh ed., McGraw-Hill, 1998.
- [9] J. Smart, R.C. Schucker, D.R. Lloyd, Pervaporative extraction of volatile organic compounds from aqueous systems with use of a tubular transverse flow module. Part I. Composite membrane study, *J. Membr. Sci.* 143 (1998) 137–157.
- [10] S. Han, L. Puech, R.V. Law, J.H.G. Steinke, A. Livingston, Selection of elastomeric membranes for the separation of organic compounds in acidic media, *J. Membr. Sci.* 199 (2002) 1–11.
- [11] L.D. Collins, A.J. Daugulis, Biodegradation of phenol at high initial concentrations in two-phase partitioning batch and fed-batch bioreactors, *Biotechnol. Bioeng.* 55 (1997) 155–162.
- [12] F. Castelo Alves Ferreira, Membrane Aromatic Recovery System: theoretical analysis and industrial applications, Ph.D. thesis, Imperial College London, 2004.
- [13] E.W. Washburn, *International Critical Tables of Numerical Data, Physics Chemistry and Technology*, first electronic ed., Knovel, 2003.
- [14] L.F. Strachan, A.G. Livingston, The effect of membrane module configuration on extraction efficiency in an extractive membrane bioreactor, *J. Membr. Sci.* 128 (1997) 231–242.
- [15] A.G. Livingston, J.P. Arcangeli, A.T. Boam, S.F. Zhang, M. Marangon, L.M. Freitas dos Santos, Extractive membrane bioreactor for detoxification of chemical industry wastes: process development, *J. Membr. Sci.* 151 (1998) 29–44.